Proc. Natl. Acad. Sci. USA
Vol. 96, pp. 5516–5521, May 1999
Cell Biology

Two distinct classes of Ran-binding sites on the nucleoporin Nup-358

(RanBP1-homologous domains/GDP-bound Ran/GTP-bound Ran/RanBP1/zinc fingers)

NABEEL R. YASEEN*† AND GÜNTER BLOBEL*‡

*Laboratory of Cell Biology, Howard Hughes Medical Institute, The Rockefeller University, New York, NY 10021; and †Department of Pathology, Weill Medical College, Cornell University, New York, NY 10021

Contributed by Günter Blobel, March 23, 1999

ABSTRACT **Nup-358 is a giant nucleoporin located at the tips of the cytoplasmic fibrils of the nuclear pore complex (NPC). Its contains four RBH (RanBP1-homologous) domains and a zinc finger domain with eight zinc finger motifs. Using three recombinant fragments of Nup-358 that comprise two of the RBH domains and the zinc finger domain, we show that both RanGDP and RanGTP bind to Nup-358 *in vitro*. The RBH domains bound either RanGDP or RanGTP. Interestingly, the zinc finger domain was found to bind RanGDP exclusively. Zinc chelation by EDTA treatment abolished the binding of RanGDP to the zinc finger domain without affecting the binding of Ran to the RBH domain. Ultrastructural studies with RanGDP-conjugated colloidal gold in digitonin-permeabilized cells showed a large number of Ran-binding sites on the cytoplasmic fibrils of the NPC. Of those, only a portion that is closer to the central axis of the NPC was sensitive to RanBP1 competition, suggesting that most of the RBH domains of Nup-358 are situated closer to the central axis of the NPC than the zinc finger domain. Thus, the RBH and the zinc finger domains of Nup-358 were identified as two different classes of Ran-binding sites with distinct, ultrastructural locations at the NPC.**

Bidirectional nuclear transport of macromolecules is mediated by a family of soluble proteins called karyopherins (1). Different karyopherins act as carriers that recognize distinct nuclear import and export signals on their cargo and mediate the interaction of cargo with the nuclear pore complex (NPC). The NPC is a large complex of proteins (nucleoporins) that spans the nuclear membrane and has filamentous projections into both the nucleus and cytoplasm (2–5). Other soluble factors, including the small GTPase Ran, p10 (also called NTF2), and the small Ran-binding protein RanBP1, help to translocate cargo–carrier complexes through the NPC and to release the cargo at its destination. The exact sequence of interactions between nucleoporins and soluble factors that result in translocation from the cytoplasmic to the nuclear side of the NPC and back are not well understood.

As with other small GTPases, Ran binds to guanine nucleotides and cycles between two forms: a GDP-bound form (RanGDP) and a GTP-bound form (RanGTP); interconversion of these two forms is thought to be involved in nuclear transport (6–8). RanBP1 binds to RanGTP (9–11) and, with lower affinity, to RanGDP (12, 13) and forms trimeric complexes with karyopherin β1 (Kapβ1) and either RanGDP or RanGTP (14, 15). Two factors regulate the interconversion of RanGTP and RanGDP. RanGAP1, located predominantly in the cytosol and the cytoplasmic surface of the NPC, is an activator of Ran GTPase activity that converts RanGTP to RanGDP. NPC-associated RanGAP1 is covalently modified by a small, ubiquitin-like molecule (SUMO-1) (16, 17). SUMO-RanGAP1 is attached to the C terminus of Nup-358 and is the only species retained in digitonin-permeabilized cells (16, 18, 19). RCC1 is a predominantly intranuclear guanine nucleotide exchange factor (GEF) for Ran that allows the release of bound nucleotide and reloading of Ran (6, 7, 20–22). Because the cellular concentration of GTP is higher than that of GDP, RCC1 is thought to favor the formation of RanGTP. Based on the cellular distribution of these two factors, it is believed that nuclear Ran is predominantly in the GTP-bound form whereas cytoplasmic Ran is mostly GDP-bound. RanGTP binds to Kapβ1, leading to the release of Kapα along with the bound cargo (23).

Nup-358 is a 358-kDa nucleoporin that is localized to the tips of the cytoplasmic fibrils of the NPC (24, 25). It has four domains homologous to RanBP1 (RBH domains), a leucine-rich region, a zinc finger region, FG and FXFG repeats characteristic of a subset of nucleoporins, and a cyclophilin-homologous domain (24, 25). It binds RanGTP in overlay and microtiter-plate assays (24–26). Ran loaded with GTP or its nonhydrolyzable analog GMP-PNP has been shown to interact with the cytoplasmic side of the NPC in rat liver nuclear envelope preparations by electron microscopy (24, 26). These findings suggest that RanGTP interacts with Nup-358 at the NPC. Nuclear import is favored when Ran is provided in its GDP-bound form and is inhibited by nonhydrolyzable analogs of GTP and mutants of Ran that do not hydrolyze GTP (26–33). Immunofluorescence microscopy reveals clear binding of RanGDP to the nuclear envelope (30); yet, overlay assays failed to detect RanGDP binding to Nup-358 (25, 26). Thus, neither the ultrastructural location nor the molecular receptor of RanGDP at the nuclear envelope is known.

Using an ultrastructural assay with gold-labeled recombinant proteins in digitonin-permeabilized cells and *in vitro* solution-binding assays with three different portions of Nup-358, we identify the nucleoporin Nup-358 as a major binding site for both RanGDP and RanGTP at the NPC. RanGDP bound to both the zinc finger and the RBH domains of Nup-358 whereas RanGTP binding was restricted to the RBH domains. Binding of Ran to the RBH domains was sensitive to competition by RanBP1 and resistant to zinc chelation, whereas binding of RanGDP to the zinc finger domain was RanBP1-resistant and sensitive to zinc chelation. Ultrastructural studies confirm the presence of at least two classes of Ran-binding sites at the tips of the cytoplasmic fibrils of the NPC. The RanBP1-senstitive sites (presumably representing RBH domains) were closer to the central axis of the NPC than the RanBP1-resistant sites. These findings show that the zinc finger domain of Nup-358 is a novel RanGDP-binding site at

The publication costs of this article were defrayed in part by page charge payment. This article must therefore be hereby marked "*advertisement*" in accordance with 18 U.S.C. §1734 solely to indicate this fact.

PNAS is available online at www.pnas.org.

Abbreviations: NPC, nuclear pore complex; RBH, RanBP1 homologous; TB, transport buffer; GST, glutathione *S*-transferase.

‡To whom reprint requests should be addressed. e-mail: blobel@rockvax.rockefeller.edu.

the NPC that is biochemically and ultrastructurally distinct from the RBH domains.

MATERIALS AND METHODS

Cell Culture and Permeabilization. HeLa cells were cultured in DMEM supplemented by 10% FCS/2 mM glutamine/100 units/ml each of penicillin and streptomycin. They were digitonin-permeabilized and stored essentially as described (34). Cells were nonenzymatically dissociated in dissociation solution (Sigma C-5914) for 15 min at 37°C and washed three times by low-speed centrifugation in cold transport buffer (TB: 20 mM Hepes, pH 7.4/110 mM potassium acetate/2 mM magnesium acetate/1 mM EGTA). They then were suspended in TB with 35 μg/ml of digitonin and incubated for 5 min on ice followed by three washes in cold TB. They were resuspended in TB with 10 mg/ml of BSA (Sigma A-7030) and 5% DMSO at 10^7 cells/ml and stored in aliquots at −80°C.

Recombinant Proteins. Human Ran was expressed in *Escherichia coli* BL21(DE3) from a pET-9C construct (9) and purified as described (35). Recombinant human Ran was loaded with either GDP or GTP as described (35) before use. The Nup-358–4 protein (18) was a kind gift from Jian Wu (The Rockefeller University). The Nup-358–1 construct was produced by amplifying the region of the Nup-358 cDNA that encodes amino acids 996-1963 from a plasmid containing the 7–4 fragment of Nup-358 (24) provided by Jian Wu. It was subcloned into pGEX4T3 and expressed as a fusion protein with glutathione *S*-transferase (GST) in *E. coli*. The Nup-358-ZF construct was made by removing the RBH1 domain from the Nup-358–1 construct by a restriction digest, filling in of the recessed ends with Klenow fragment, and religating the ends. Recombinant RanBP1, expressed from a pET11 construct [kindly provided by Elias Coutavas (The Rockefeller University)] was a gift from Yuh-Min Chook and Tschong-Uk Park (The Rockefeller University).

Conjugation of Recombinant Ran to Colloidal Gold Particles. The optimum amount of recombinant protein needed to stabilize colloidal gold beads (BB International, Cardiff, U.K.) was determined by titration according to the manufacturer's instructions. Colloidal gold beads, 5 nm in diameter, were incubated with the recombinant protein for 5 min at room temperature and brought up to pH 9 with 0.2 M potassium carbonate. BSA was added to 10 mg/ml, and the coated beads were then concentrated 50-fold by centrifugation according to the manufacturer's instructions. Gold conjugates were checked by electron microscopy to ensure that the preparation was monodisperse with no clumping of gold particles.

Electron Microscopy. Approximately 5×10^4 digitonin-permeabilized HeLa cells were incubated with 2 μl of 5-nm gold conjugate for 40 min at 22°C in 30 μl TB followed by overnight fixation in 5% glutaraldehyde at 4°C. Samples were processed for transmission electron microscopy and viewed with a JEOL 100CX microscope. Two photographs per cell were taken from ultrathin sections at ×26,000 magnification from 5–6 cells for each experimental point. For surface views of Ran-labeled NPCs, grazing sections of nuclei were photographed at ×33,000 magnification in semithin sections. Measurements of the distance of gold particles from the midplane of the NPC were carried out in ultrathin sections photographed at ×26,000 magnification. All electron micrographs were scanned and saved by using Adobe PHOTOSHOP 4.0 software. Quantitative analysis of the images to determine the number and distance of gold particles from the midplane of the NPC was carried out with NIH IMAGE 1.61 software.

***In Vitro* Binding Assays.** Binding reactions contained 10 μl glutathione-Sepharose beads (Pharmacia) in a total volume of 46 μl in transport buffer with Tween 20 (TB-T: 20 mM Hepes, pH 7.4/110 mM potassium acetate/2 mM magnesium chloride/0.1% Tween 20) and 0.5 mg/ml of Pefabloc SC (Boehringer Mannheim). Nup-358–1, Nup-358–4, and Nup-358-ZF were present at 0.25 μM each; Ran was at 0.8 μM. Reactions were allowed to proceed for 1 h at 4°C with rotation. After centrifugation, the supernatant was collected and the beads were washed twice in cold TB-T. The bound and unbound fractions were subjected to SDS/PAGE on 5–20% gradient gels. Proteins were visualized by Coomassie blue staining of gels, Amido black staining of blots, or Western blotting as indicated in the text and figure legends. In Western blots, Ran was detected by using a polyclonal rabbit antibody (27) followed by horseradish peroxidase-conjugated secondary antibody. Detection was by chemiluminescence using SuperSignal reagents (Pierce). For binding experiments with radioactively labeled RanGDP and RanGTP, Ran was labeled with either [β-^{32}P]GDP or [γ-^{32}P]GTP as described (35). Binding reactions and washing were carried out as described above for nonradioactive Ran, and radioactivity bound to the beads was measured in a scintillation counter. Removal of zinc from the zinc finger domains of Nup-358–1 was carried out by washing Nup-358–1 or Nup-358-ZF immobilized on glutathione-Sepharose beads twice with a buffer containing 50 mM EDTA/100 mM sodium acetate/0.1% Tween 20, pH 5.5, followed by overnight incubation in the same buffer. The beads then were washed three times in the same buffer and five times with TB-T. As a control, Nup-358–1 beads were treated by undergoing the same series of incubations and washes in TB-T instead of EDTA-containing buffer.

RESULTS

Nup-358 Binds Both RanGDP and RanGTP. The nucleoporin Nup-358, located at the cytoplasmic fibrils of the NPC, contains a leucine-rich region, four domains that are homologous to RanBP1 (RBH domains), a region of eight zinc fingers, a cyclophilin-homologous domain, and scattered FG repeats that are characteristic of a subset of nucleoporins (24, 25) (Fig. 1). The presence of RBH sites on Nup-358 suggests that it may provide Ran-binding sites during nuclear transport. Indeed, in overlay and microtiter plate assays Nup-358 has been shown to bind RanGTP (24–26). However, these studies did not demonstrate binding of RanGDP to Nup-358 in spite of the fact that RanGDP binds to the nuclear envelope and is needed for import of NLS-bearing cargo (30, 33). It was therefore important to test whether binding of RanGDP to Nup-358 could be detected in solution-binding assays.

Two recombinant fragments of Nup-358, named Nup-358–1 and Nup-358–4, were expressed in *E. coli* as fusion proteins with an N-terminal GST tag. The Nup-358–1 fragment contains the RBH1 domain, the eight zinc fingers, and several FG repeats, whereas the Nup-358–4 fragment contains the RBH4 domain, the cyclophilin-homologous domain, and several FG repeats (Fig. 1). The two fragments were immobilized on glutathione-Sepharose beads, and each was incubated with RanGDP or RanGTP. The bound and unbound fractions were analyzed by SDS/PAGE. As expected, both Nup-358 fragments bound RanGTP (Fig. 2). In addition, however, both fragments also bound RanGDP, more prominently in the case of Nup-358–1 (Fig. 2). These data suggest that Nup-358 provides binding sites for both RanGDP and RanGTP at the NPC.

The RBH and Zinc Finger Domains Are Two Distinct Types of Ran-Binding Sites on Nup-358. To determine whether Ran binding to the two Nup-358 fragments is mediated by the RBH domains, we carried out competition experiments. Binding of Ran to the RBH domain of either Nup-358–1 and Nup-358–4 should be competed by RanBP1. When the immobilized Nup-358–4 fragment was incubated with RanGDP or RanGTP in the presence of increasing concentrations of RanBP1, binding of Ran was almost completely abolished (see immunoblot in Fig. 3*B*), which is consistent with Ran binding to the RBH4 domain. In contrast, there was only partial

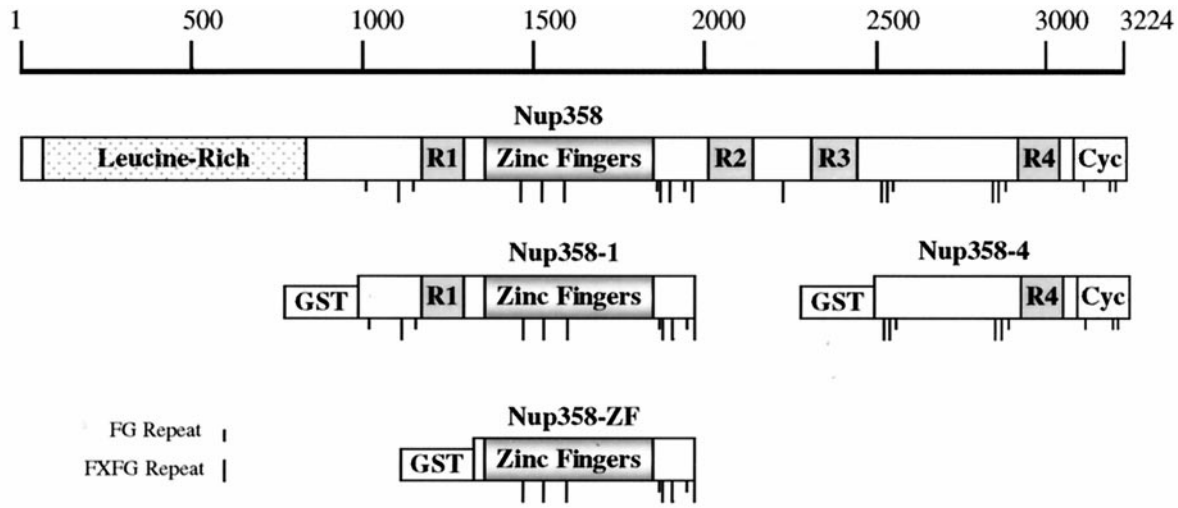

FIG. 1. Schematic diagrams of Nup-358 (24, 25) and the three GST-fusion constructs used in this study, Nup-358–1, Nup-358–4, and Nup-358-ZF. R1–4, RBH domains 1–4; Cyc, cyclophilin-homologous domain. Numbers on the scale indicate amino acid positions.

competition for Ran binding to the Nup-358–1 fragment, even at the highest concentration of RanBP1 (Fig. 3*A*).

This suggests that there are two distinct binding sites for Ran on the Nup-358–1 fragment: one sensitive to RanBP1 competition, presumably the RBH1 domain, and one resistant to RanBP1 competition. The major feature present in Nup-358–1 and absent from Nup-358–4 is the zinc finger domain (Fig. 1). Zinc fingers mediate protein interactions with DNA, RNA, and with other proteins (36). An interaction between the zinc fingers of Nup-358–1 and Ran therefore could account for the RanBP1-resistant portion of Ran binding to the Nup-358–1 fragment. The amounts of RanGDP or RanGTP that bound to Nup-358–1 (Fig. 2 *Left*) suggested that if the zinc finger region is indeed a Ran-binding domain, it might be able to bind both RanGDP and RanGTP. Because RanGTP preparations also contain some RanGDP and *vice versa* (35), we used RanGDP containing ^{32}P in the β position and RanGTP containing ^{32}P in the γ position to further characterize binding of Ran to Nup-358–1.

Removal of zinc from zinc fingers results in loss of their normal binding properties (37, 38). Thus, if the zinc finger domain indeed represents a Ran-binding site, then removal of zinc should abolish binding of Ran to the zinc finger domain of Nup-358–1 without affecting the Ran-binding ability of its RBH1. Removal of zinc from zinc finger-containing proteins can be accomplished by chelation with EDTA at an acidic pH (37, 39). Therefore, to assess the effect of zinc chelation on

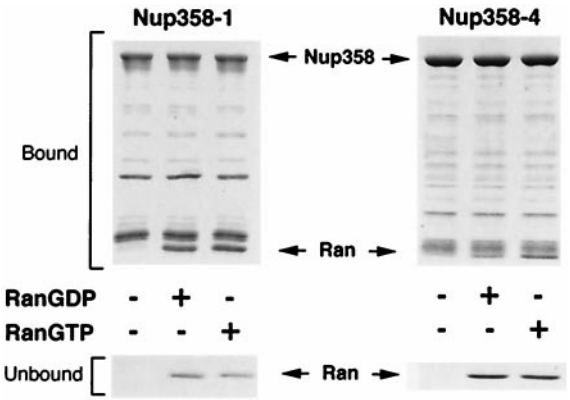

FIG. 2. Nup-358 binds to both RanGDP and RanGTP. Glutathione-Sepharose beads with immobilized Nup-358–1 (*Left*) or Nup-358–4 (*Right*) at 0.25 μM were incubated with 0.8 μM RanGDP or RanGTP. Bound and unbound fractions were visualized by SDS/PAGE and Coomassie blue staining.

Ran binding, immobilized Nup-358–1 was preincubated with 50 mM EDTA to chelate zinc and then washed with buffer to remove traces of EDTA.

Immobilized Nup-358–1 (with or without EDTA treatment) was incubated with either [γ-^{32}P]RanGTP or [β-^{32}P]RanGDP in the absence or presence of RanBP1, and the percentage of radioactivity bound to the beads was measured (Fig. 4). All of the [γ-^{32}P]RanGTP binding to Nup-358–1 was abolished by RanBP1, and none of it was affected by EDTA treatment (Fig. 4*A*). This indicates that RanGTP binds exclusively to the RBH domain of Nup-358–1. In contrast, the binding of [β-^{32}P]RanGDP to Nup-358–1 was partially competed away by RanBP1, suggesting that only part of the RanGDP was bound to the RBH domain (Fig. 4*B*). Furthermore, EDTA-treated Nup-358–1 showed reduced binding to RanGDP, and the vast majority of that binding was now abolished by RanBP1 (Fig. 4*B*). The reduction of RanGDP binding after EDTA treatment is unlikely to be due to nonspecific denaturation of the protein, because RanGTP binding under the same conditions was unaffected (Fig. 4*A*). These data are consistent with the presence of two RanGDP-binding sites on Nup-358–1: the RanBP1-sensitive RBH domain and the EDTA-sensitive zinc finger domain.

To confirm that the zinc finger domain of Nup-358 is indeed a RanGDP-binding site, a fragment containing only the zinc finger domain of Nup-358 (Nup-358-ZF) was expressed in *E. coli* as a GST-fusion protein (Fig. 1). Binding assays with immobilized Nup-358-ZF and either RanGDP or [β-^{32}P]RanGDP were carried out as described above. As shown in Fig. 5, Nup-358-ZF bound to RanGDP and the binding was almost completely abolished by EDTA treatment as seen by Coomassie blue staining (Fig. 5*A*) and by radioactivity counts (Fig. 5*B*).

Taken together these data show that the zinc finger domain of Nup-358 is a zinc-dependent RanGDP-binding site, whereas the RBH domains of Nup-358 bind either RanGDP or RanGTP in a RanBP1-sensitive fashion.

Ultrastructural Localization of Ran-Binding Sites on the NPC. To test whether these *in vitro* solution-binding data reflect events occurring on intact NPCs, we incubated RanGDP coupled to 5-nm colloidal gold with digitonin-permeabilized cells. Electron microscopic inspection of sections of these cells showed that RanGDP coupled to gold yielded extensive labeling at the cytoplasmic side of the NPC (Fig. 6*A*). The great majority of the RanGDP-gold particles was found at a distance of 35–60 nm from the midplane of the NPC (Fig. 6*B*), which is consistent with binding to Nup-358

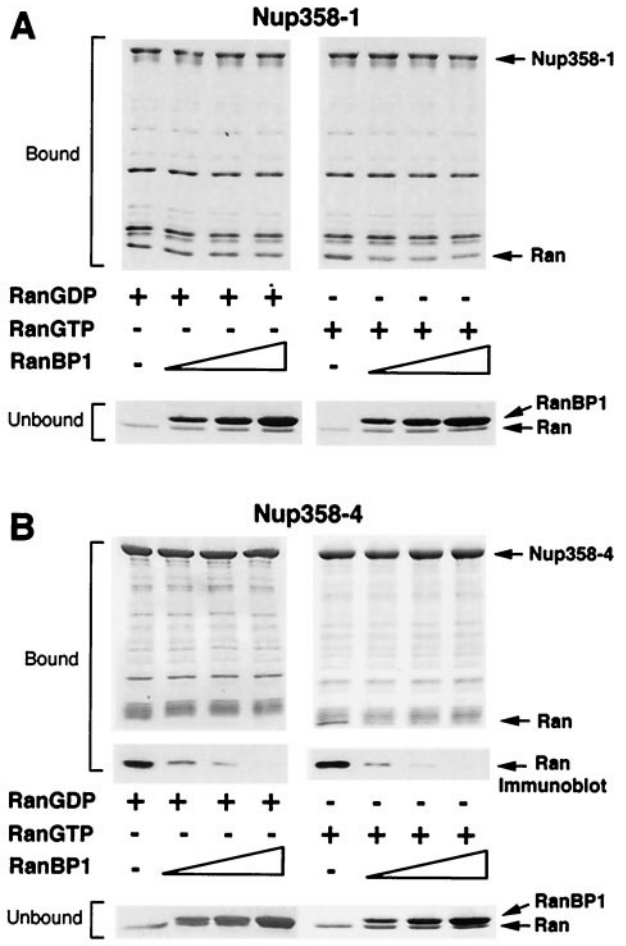

FIG. 3. RanBP1 competes with Nup-358–4 and, partially, with Nup-358–1 for Ran binding. (*A*) Glutathione-Sepharose beads with immobilized 0.25 μM Nup-358–1 were incubated with 0.8 μM RanGDP or RanGTP as indicated in the presence or absence of 1, 2, or 4 μM RanBP1. Bound and unbound fractions were visualized by SDS/PAGE and Coomassie blue staining. (*B*) Glutathione-Sepharose beads with immobilized 0.25 μM Nup-358–4 were incubated with 0.8 μM RanGDP or RanGTP as indicated in the presence or absence of 1, 2, or 4 μM RanBP1. Bound and unbound fractions were visualized by SDS/PAGE and Coomassie blue staining (*Right*) or Amido black staining after transfer to nitrocellulose membrane (*Left*). Ran also was visualized by immunoblotting with rabbit polyclonal Ran antibody (27) where indicated.

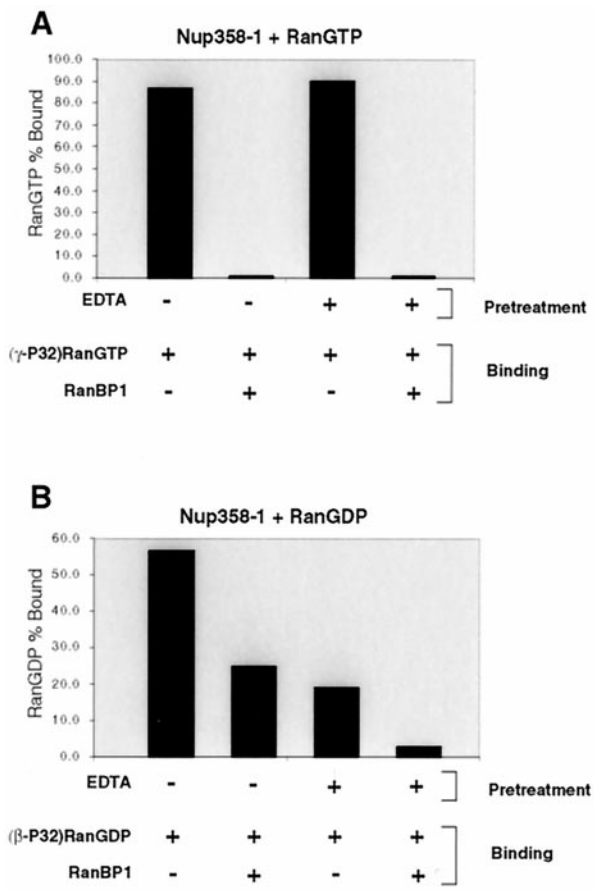

FIG. 4. RanBP1 completely abolishes RanGTP binding to Nup-358–1 whereas inhibition of RanGDP binding requires both zinc chelation and RanBP1. Binding reactions with Nup-358–1 immobilized on beads were carried out as in Fig. 3 but with [β-^{32}P]RanGDP or [γ-^{32}P]RanGTP. (*A*) Nup-358–1, either untreated or EDTA-treated (see *Materials and Methods*), was incubated with [γ-^{32}P]RanGTP in the presence or absence of 4 μM RanBP1. (*B*) Binding assays were performed as in *A* except that [β-^{32}P]RanGDP was used instead of [γ-^{32}P]RanGTP. Bound radioactivity was measured and expressed as a percentage of total Ran-associated radioactivity in the reaction.

(24). Ran-gold particles often could be seen decorating the NPC in striking rows of several gold particles, particularly in *en face* views, with up to 83 RanGDP-gold particles per NPC (Fig. 6*C Left*). Interestingly, the abundant decoration of gold particles in *en face* views of the NPC was reduced significantly and became restricted to the periphery of the NPC when incubation with Ran-gold was carried out in the presence of RanBP1 (Fig. 6*C Right*). Similar binding patterns were observed with RanGTP-conjugated gold but with more gold labeling at the center of the NPC in en face views (unpublished data).

These data are entirely consistent with the solution-binding data shown in Figs. 2–5. The extensive labeling of the NPC by Ran-gold in string-like patterns most likely reflects binding to the four RBH domains and the zinc finger domains of Nup-358. The gold particles in the periphery of the NPC that were not competed by RanBP1 are likely to be those decorating the zinc finger domains of Nup-358.

DISCUSSION

In Figs. 2–5, we use *in vitro* binding assays to show that Nup-358 binds to both RanGDP and RanGTP and that two distinct sites on Nup-358 are involved in this binding. The zinc finger domain is a novel Ran-binding site that binds RanGDP exclusively, is zinc-dependent, and is resistant to RanBP1 competition, whereas the RBH domain binds both RanGDP and RanGTP, is not affected by zinc depletion, and is sensitive to RanBP1 competition.

Previous studies using overlay assays showed binding of RanGTP to Nup-358 (24–26) but did not demonstrate binding of RanGDP to Nup-358 (25, 26). Failure of overlay assays to detect the binding of RanGDP to Nup-358 is not surprising; binding of RanGDP and a Ran mutant to RanBP1 (12, 13) also was missed initially by overlay assays (9, 10). This may be due to a reduced sensitivity and/or the fact that proteins are denatured and affixed to a membrane in these assays.

Ultrastructural studies using gold-conjugated Ran confirm the *in vitro* results and shed some light on the topology of Nup-358 and the number of Ran-binding sites at the NPC. An average of 64 RanGDP-gold particles were observed per NPC with as many as 83 particles on some NPCs (Fig. 6*C*). This number is much larger than that obtained in a previous study using isolated rat liver nuclear envelopes and RanGTP conjugated to 10-nm gold (24). This probably is due to the larger size of gold particles used; other possible contributing factors include the harsher nature of nuclear envelope preparation

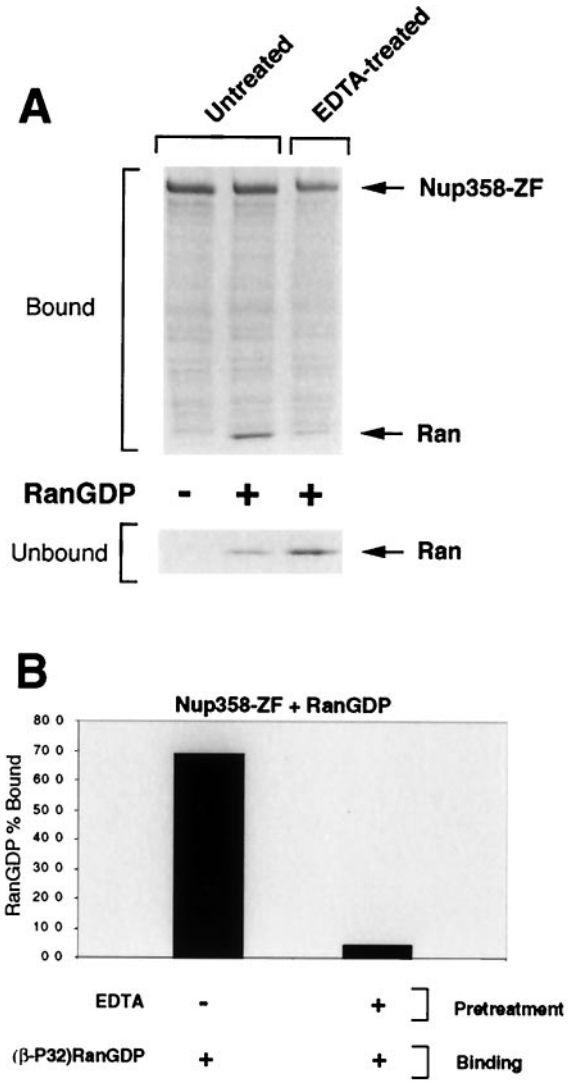

FIG. 5. The zinc finger domain of Nup-358 binds to RanGDP, and binding is prevented by zinc chelation. (*A*) Immobilized Nup-358-ZF protein (see Fig. 1), either untreated or EDTA-treated, was incubated with or without RanGDP. Bound and unbound fractions were visualized by SDS/PAGE and Coomassie blue staining. (*B*) Immobilized Nup-358-ZF protein, either untreated or EDTA-treated, was incubated with [β-^{32}P]RanGDP. Bound radioactivity was measured and expressed as a percentage of total Ran-associated radioactivity in the reaction.

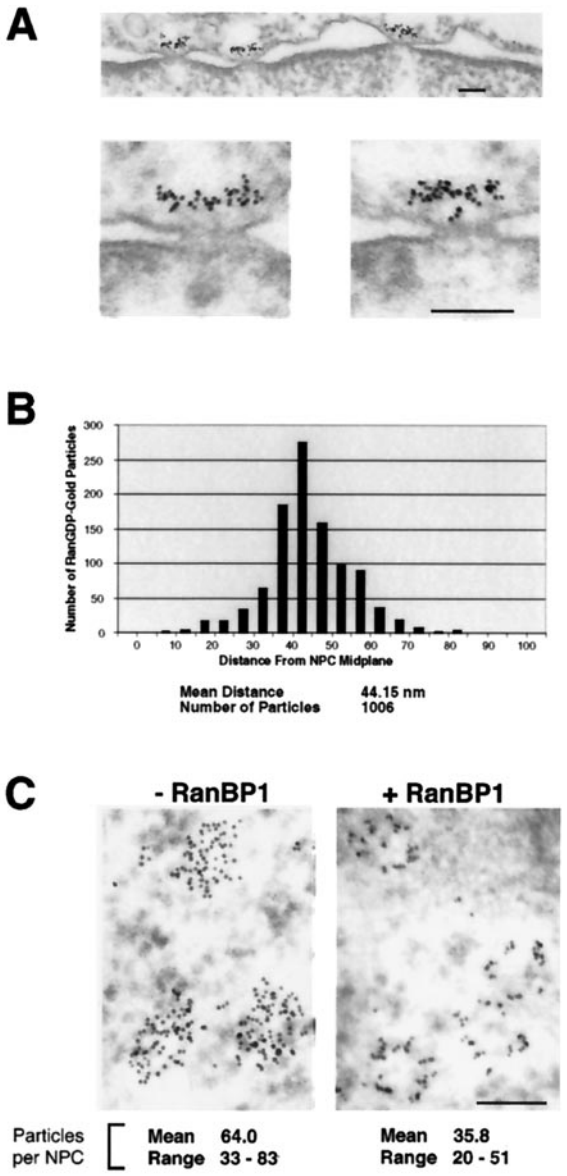

FIG. 6. Numerous binding sites for Ran on the cytoplasmic fibrils of the NPC, partially competed away by RanBP1. (*A*) Vertical sections. RanGDP binds to the cytoplasmic fibrils of the NPC in large numbers. RanGDP was conjugated to 5-nm gold beads and incubated with digitonin-permeabilized HeLa cells as described in *Materials and Methods*. Vertical ultra-thin sections through several NPCs were photographed at an original magnification of ×26,000 (*Left*). (Bars = 100 μm.) (*B*) Distance of RanGDP-gold particles from the midplane of the NPC. Photographs of vertical sections through 25 NPCs obtained as in *A* were analyzed by using Adobe PHOTOSHOP and NIH IMAGE software to determine the distance of RanGDP 5-nm gold particles from the midplane of the NPC. (*C*) Surface views. RanBP1 competes away a substantial portion of RanGDP, leaving a peripheral ring of RanGDP bound to the NPC. RanGDP was conjugated to 5-nm gold beads and incubated with digitonin-permeabilized HeLa cells as in *A* in the presence (*Right*) or absence (*Left*) of 4 μM RanBP1. Grazing sections parallel to the surface of the nucleus were photographed in semithin sections at ×33,000 original magnification. RanGDP-gold particles were counted in 23 and 27 NPCs in the absence and presence of RanBP1, respectively. (Bar = 100 μm.)

compared with digitonin permeabilization and the reaction conditions used. Yet, it is unlikely that all Ran-binding sites at the NPC would be decorated even with 5-nm gold particles in digitonin-permeabilized cells. One reason is that some endogenous Ran remains bound to the NPC in digitonin-permeabilized cells (40). Furthermore, the process of gold conjugation and the bulk of the gold particle itself is likely to preclude binding to some available Ran-binding sites. Finally, the multivalent nature of gold conjugates raises the possibility that one particle may bind to more than one site simultaneously. Thus, 83 is likely to be a low estimate of the actual number of Ran-binding sites at the NPC.

A portion of the RanGDP-gold particles bound to the cytoplasmic fibrils of the NPC is competed away by RanBP1 (Fig. 6*C*), which is consistent with the interaction of Ran with RBH domains on Nup-358. The number of particles competed away by RanBP1, estimated by subtracting the average number of gold particles bound in the presence of RanBP1 from that bound in the absence of RanBP1, is 28.2 (Fig. 6*C*). Bearing in mind the limitations of quantitation discussed above, this number should give a rough indication of the number of RBH domains on the NPC. The 8-fold symmetry of the NPC suggests a minimum of 8 molecules of Nup-358 per NPC. With 4 RBH domains per Nup-358 molecule, this implies 32 RBH

domains per NPC—a number remarkably close to the experimental estimate of 28.2.

Some of the Ran remains on the cytoplasmic fibrils at the periphery of the NPC in the presence of RanBP1, forming a ring-like pattern (Fig. 6*C*). This most likely represents binding to the zinc finger domain of Nup-358 and would predict that this domain is situated closer to the periphery of the NPC than the bulk of the RBH domains. This suggests that the orientation of Nup-358, at least in permeabilized cells, has a horizontal component that stretches from the periphery to the central axis of the NPC. The average number of RanGDP-gold particles bound to the NPC in the presence of RanBP1 is 35.8, with some NPCs decorated with as many as 51 particles (Fig. 6*C*). For the reasons discussed above, even 51 may be an underestimate of the actual number of non-RBH Ran-binding sites on the NPC. However, the possibility that some of this binding is due to non-RBH Ran-binding sites on nucleoporins other than Nup-358 cannot be excluded. Thus, the number of RanGDP-binding sites on the zinc finger domain of Nup-358 would be difficult to predict from these data. The function of RanGDP that is bound to the zinc finger domain of Nup-358 is not clear. Because RanGDP appears to be a required intermediate in nuclear import (30, 33), it is possible that the zinc fingers may serve to provide a high local concentration of RanGDP at the NPC.

This work would not have been possible without the expert assistance of Helen Shio from the Rockefeller University electron microscopy facility. We are grateful to Jian Wu, Yuh-Min Chook, Tschong-Uk Park, and Elias Coutavas for valuable reagents. We would also like to thank Jonathan Rosenblum for critical reading of the manuscript and members of the Blobel lab for many helpful discussions. N.R.Y. is supported by the K08 CA72959 award from the National Institutes of Health.

1. Pemberton, L. F., Blobel, G. & Rosenblum, J. S. (1998) *Curr. Opin. Cell Biol.* **10,** 392–399.
2. Bastos, R., Pante, N. & Burke, B. (1995) *Int. Rev. Cytol.* **162B,** 257–302.
3. Doye, V. & Hurt, E. (1997) *Curr. Opin. Cell Biol.* **9,** 401–411.
4. Yang, Q., Rout, M. P. & Akey, C. W. (1998) *Mol. Cell* **1,** 223–234.
5. Ohno, M., Fornerod, M. & Mattaj, I. W. (1998) *Cell* **92,** 327–336.
6. Rush, M. G., Drivas, G. & D'Eustachio, P. (1996) *BioEssays* **18,** 103–112.
7. Moore, M. S. (1998) *J. Biol. Chem.* **273,** 22857–22860.
8. Cole, C. N. & Hammell, C. M. (1998) *Curr. Biol.* **8,** R368–R372.
9. Coutavas, E., Ren, M., Oppenheim, J. D., D'Eustachio, P. & Rush, M. G. (1993) *Nature (London)* **366,** 585–587.
10. Lounsbury, K. M., Beddow, A. L. & Macara, I. G. (1994) *J. Biol. Chem.* **269,** 11285–11290.
11. Bischoff, F. R., Krebber, H., Smirnova, E., Dong, W. & Ponstingl, H. (1995) *EMBO J.* **14,** 705–715.
12. Richards, S. A., Lounsbury, K. M. & Macara, I. G. (1995) *J. Biol. Chem.* **270,** 14405–14411.
13. Kuhlmann, J., Macara, I. & Wittinghofer, A. (1997) *Biochemistry* **36,** 12027–12035.
14. Chi, N. C., Adam, E. J., Visser, G. D. & Adam, S. A. (1996) *J. Cell Biol.* **135,** 559–569.
15. Lounsbury, K. M. & Macara, I. G. (1997) *J. Biol. Chem.* **272,** 551–555.
16. Matunis, M. J., Coutavas, E. & Blobel, G. (1996) *J. Cell Biol.* **135,** 1457–1470.
17. Mahajan, R., Delphin, C., Guan, T., Gerace, L. & Melchior, F. (1997) *Cell* **88,** 97–107.
18. Matunis, M. J., Wu, J. & Blobel, G. (1998) *J. Cell Biol.* **140,** 499–509.
19. Mahajan, R., Gerace, L. & Melchior, F. (1998) *J. Cell Biol.* **140,** 259–270.
20. Avis, J. M. & Clarke, P. R. (1996) *J. Cell Sci.* **109,** 2423–2427.
21. Seki, T., Hayashi, N. & Nishimoto, T. (1996) *J. Biochem. (Tokyo)* **120,** 207–214.
22. Koepp, D. M. & Silver, P. A. (1996) *Cell* **87,** 1–4.
23. Rexach, M. & Blobel, G. (1995) *Cell* **83,** 683–692.
24. Wu, J., Matunis, M. J., Kraemer, D., Blobel, G. & Coutavas, E. (1995) *J. Biol. Chem.* **270,** 14209–14213.
25. Yokoyama, N., Hayashi, N., Seki, T., Pante, N., Ohba, T., Nishii, K., Kuma, K., Hayashida, T., Miyata, T., Aebi, U., *et al.* (1995) *Nature (London)* **376,** 184–188.
26. Melchior, F., Guan, T., Yokoyama, N., Nishimoto, T. & Gerace, L. (1995) *J. Cell Biol.* **131,** 571–581.
27. Moore, M. S. & Blobel, G. (1993) *Nature (London)* **365,** 661–663.
28. Moore, M. S. & Blobel, G. (1994) *Proc. Natl. Acad. Sci. USA* **91,** 10212–10216.
29. Melchior, F., Paschal, B., Evans, J. & Gerace, L. (1993) *J. Cell Biol.* **123,** 1649–1659.
30. Gorlich, D., Pante, N., Kutay, U., Aebi, U. & Bischoff, F. R. (1996) *EMBO J.* **15,** 5584–5594.
31. Schlenstedt, G., Saavedra, C., Loeb, J. D., Cole, C. N. & Silver, P. A. (1995) *Proc. Natl. Acad. Sci. USA* **92,** 225–229.
32. Palacios, I., Weis, K., Klebe, C., Mattaj, I. W. & Dingwall, C. (1996) *J. Cell Biol.* **133,** 485–494.
33. Weis, K., Dingwall, C. & Lamond, A. I. (1996) *EMBO J.* **15,** 7120–7128.
34. Gorlich, D., Prehn, S., Laskey, R. A. & Hartmann, E. (1994) *Cell* **79,** 767–778.
35. Floer, M. & Blobel, G. (1996) *J. Biol. Chem.* **271,** 5313–5316.
36. Mackay, J. P. & Crossley, M. (1998) *Trends Biochem. Sci.* **23,** 1–4.
37. Pan, T. & Coleman, J. E. (1989) *Proc. Natl. Acad. Sci. USA* **86,** 3145–3149.
38. Predki, P. F. & Sarkar, B. (1992) *J. Biol. Chem.* **267,** 5842–5846.
39. Craig, T. A., Veenstra, T. D., Naylor, S., Tomlinson, A. J., Johnson, K. L., Macura, S., Juranic, N. & Kumar, R. (1997) *Biochemistry* **36,** 10482–10491.
40. Moore, M. S. & Blobel, G. (1995) *Cold Spring Harbor Symp. Quant. Biol.* **60,** 701–705.